Strength of textile composites – A voxel based continuum damage mechanics approach

Raimund Rolfes[1], Gerald Ernst[1], Daniel Hartung[2], and Jan Teßmer[2]

[1] Institute for Structural Analysis, University of Hannover
Appelstraße 9a, 30167 Hannover, Germany
{r.rolfes, g.ernst}@isd.uni-hannover.de
[2] Institute of Composite Structures and Adaptive Systems, DLR Braunschweig
Lilienthalplatz 7, 38108 Braunschweig, Germany
{jan.tessmer, daniel.hartung}@dlr.de

For the prediction of composite strengths with representative volume elements (RVE) a thorough understanding of the ongoing failure mechanisms is needed. This again is influenced by the manufacturing process. Therefore, a brief overview on fabrication, material characteristics and failure mechanisms for Prepreg and textile composites is given in the present paper. For the strength analysis two RVE approaches, one for Prepreg and one for textile composites, are illustrated. The RVE approach on UD-laminae is used for calibration of the textile composites RVE. Two material models are compared.

1 Introduction

For stiffness of UD-laminae analytical RVE calculations and rules of mixture are state of the art, see e.g. [5]. Strengths nonetheless are mostly determined by testing.

For textile composites finite element RVE computations play a major role in the prediction of strength , see Sects. 3.2 and 3.3. In contrast to analytical methods they allow for consideration of the spatial fibre architecture. A special RVE approach based on voxel discretisation and continuum damage mechanics is developed. For calibration purposes, this approach is applied to a single UD-lamina and compared with experimental results of the World-Wide Failure Exercise (WWFE) by Hinton et al. [9]. Then the method is applied to a special class of textile composites (NCF) with the objective to qualify an engineering failure criterion. Recent research activities on strength of textile composites are given in Sect. 3.2.

2 Pre impregnated Composites (Prepreg)

Generally composites are available in form of a dry textile, which has to be impregnated with resin during the fabrication process, and in form of a semi finished

resin-fibre material, which is already soaked with resin. The latter consists of pre-impregnated fibres, also known as prepreg, and is commonly used to produce high quality composite parts, in particular for aerospace industry.

Compared to textiles composites, where resin is directly infused into the component or structure, the resin in prepreg is impregnated during the material fabrication. Therefore textiles are able to be stored under ordinary environmental conditions, whereas prepregs have to be stored in cold conditions in a freezed form to prevent the curing of the resin. However, prepreg systems are more relevant for high performance structures due to their advantageous material properties compared with textiles. The reinforcement fibres are aligned in a precise, continuous direction and provide an optimal structural performance of the material. Nearly all fibre materials (Carbon, Glas, Aramid) are available for prepregs.

2.1 Fabrication and material characteristic of Prepreg Composites

In principle the material behaviour and fabrication of prepreg is significantly different from textile composites. However, prepreg composites provide a very high material quality and reproducibility.

2.1.1 Fabrication

Usually the prepreg is delivered in a ”wet” form, in which the fibres are impregnated with resin and cured to a sticky, not fully cured, form. The prepregs are usually cut into the desired shape manually or by automatic cutting. The laminate is build by stacking single plies on a tool, which is used to assure that the required component geometry is provided after curing of the resin. To prevent voids and gas or air inclusions, the laminate is evacuated by a vacuum and afterwards cured in an autoclave in order to compact the material. This process assures high reproducible material quality, high fibre volume fraction and optimal fibre alignment.

According to a cost efficient production a highly automated manufacturing procedure is commonly used in industry for producing large structural parts. However, this process is usually restricted to slightly curved geometries. Nevertheless, due to expensive material and storage conditions, manufacturing of prepreg is generally more expensive compared with textile composites. Integrated components are more difficult to manufacture and a possible disadvantageous structural performance arises from connecting differently fabricated components in one structure.

2.1.2 Material characteristics

Prepregs are characterised by an optimal fibre alignment and provide, beside wound composites, the highest potential for optimised lightweight constructions with fibre reinforced plastics. The disadvantages are rather representative for all laminated composites.

Due to different thermal expansion of resin and fibre, residual thermal stresses arise on the microscopic level after curing. It is assumed that these stresses are partly

decreased by moisture absorption of the composite under environmental conditions but they are potentially able to imply microstructural cracks. Alternating lamina orientations cause inhomogeneous stress distributions and stress peaks at the free edges already under unidirectional loads. This effect is commonly known as the free-edge effect and significantly restricts the validity of tensile material tests on coupon level. Generally, for industrial components a quasi-isotropic stacking sequence is used to minimise stress peaks between different lamina directions.

2.2 Failure characteristic

The failure characteristic of composites is complex and based on different anisotropic effects. According to the classical laminate theory it is commonly assumed that a first failure in a single lamina simply reduces the overall stiffness, whereas the laminate is able to withstand further monotonic load increase until the last lamina fails. This simple approach is commonly known as the first-ply and last-ply failure.

The failure process on the laminae level is further simplified by a separation in fibre failure (FF) and failure of the resin, sometimes known as inter-fibre failure (IFF). The nearly perfect transversely-isotropic material symmetry of prepregs is partly used by certain authors to determine additional fracture modes, for example Puck [17] defines different modes for inter-fibre failure (Fig. 1). Beyond this failure modes, the free-edge effect enables a critical delamination failure especially for prepreg composites, in which a single ply is separated from the laminate.

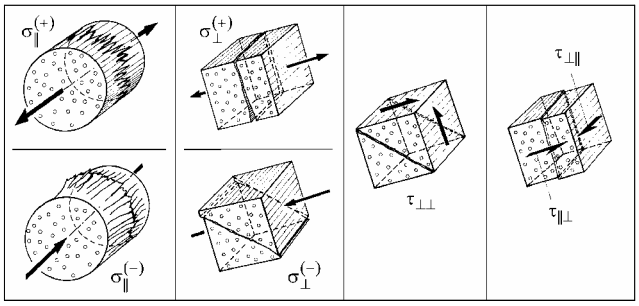

Fig. 1. Fibre and inter-fibre failure modes (Puck [17])

It is commonly assumed that the material behaviour of a carbon fibre reinforced unidirectional laminate is linear elastic up to first-ply failure. The stress-strain curve of a tensile load in fibre direction is similar to a brittle material failure. But this does not allow for the assumption that brittle material behaviour is given for all load cases. The deformation of a single lamina under compressive or shear load exhibits a non-linear behaviour (Fig. 2).

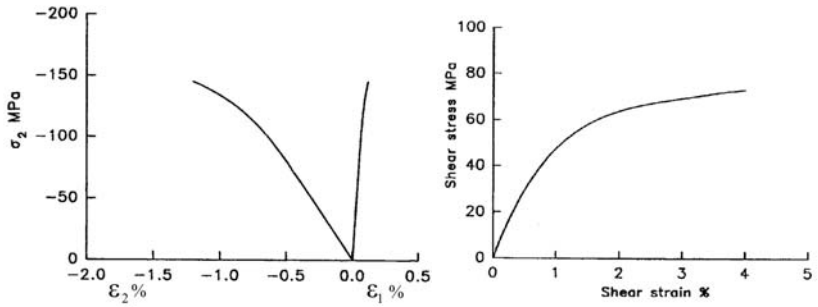

Fig. 2. Nonlinear material behaviour under transverse compression(left) and in-plane shear (WWFE[9])

2.3 Failure criteria for Prepregs

The predictive capabilities of a number of failure theories for composite laminates were compared in the World-Wide-Failure-Exercise (WWFE) [9]. Generally the failure of composites is based on an anisotropic, non-linear material behaviour, influenced by additional conditions like thermal stresses, moisture absorption, laminate lay-up, etc.. Most of the theories evaluated during the WWFE base on three different characteristic failure approximations.

The maximum-stress or -strain criterion predicts failure if a certain single stress or strain limit is reached. The strength properties are determined by testing transversely-isotropic single plies. The classical laminate theory is used to consider the material failure of a laminate. Basically, this failure prediction overestimates the failure of a lamina by multiaxial, in-plane loads.

The tensor-polynomial criteria (e.g. Tsai-Wu) consider stress interactions and transversely-isotropic strength properties. Although the failure prediction provides accurate results for combined tensile loadings, under multi-axial, in-plane compressive loads the material strength is significantly overestimated.

Certain theories are trying to predict the failure on a specific fracture plane (e.g. Puck [17]). Thus they provide the possibility to separate different fracture modes for inter-fibre failure (Fig. 1). These criteria require extensive experimental results to define the material properties and different failure criteria for tensile and compressive loads have to be considered. Therefore, they provide a relatively accurate failure approximation for multiaxial, in-plane loads.

2.4 Micromechanical analysis of UD-layer

Material properties of UD-lamina are described with the mechanical model of a representative volume element (RVE). Therefore the lamina is assumed to be arranged regularly, free of defects and residual thermal stresses. For simplicity only a single lamina is examined, to avoid the consideration of further nonlinearities, that occur in a laminate as described in Sect. 2.2. In the WWFE [9] material parameters for

four UD-laminae are given. The Silenka E-Glass 1200 tex / MY750/HY917/DY063 epoxy prepreg is chosen for the RVE analysis, see tables 2 and 3. In contrast, material parameters for textile composites are difficult to determine experimentally. Therefore this computational procedure shall be calibrated through the comparison with test results of prepreg composites for further application on textile composites.

To compute strengths of RVEs continuum damage mechanics (CDM) is applied. The necessity of the application of such sophisticated methods is described in Sect. 2.4.3. Fracture mechanics is an alternative approach, but requires an initial crack position. Such a position is not known therefore fracture mechanics are not considered for this problem. Softening of material properties causes numerical instabilities. A dynamic analysis or different regularisation techniques can be applied in such a case.

2.4.1 Computational Models

The glass fibres are assumed to be isotropic and linear elastic. For the nonlinear behaviour of the epoxy two different material models are compared subsequenty. The behaviour itself is not specified in detail in the WWFE, only initial modulus, tensile failure strain, tensile and compressive strength are given, see table 2. Based on these parameters the employed materials were approximated, see Fig. 3. In table 1 a brief overview of the material models is given, the models are shortly discussed in what follows.

Table 1. Main Differences between Models A and B

Properties	Model A	Model B
Time Integration	Explicit	Implicit
Numerical Stabilisation	dynamic terms	viscoelastic regularisation
Damage evolution depends on	fracture energy	strain energy
Material degradation	plastic, with hardening	damage variable

Model A: Quasi-static analysis with fracture energy approach

The first approach is a standard damage model from the finite element program ABAQUS. An elasto-plastic material combined with isotropic hardening and isotropic damage is used to model the nonlinear behaviour and the failure of the epoxy matrix material. The damage evolution is defined in terms of the fracture energy dissipation G_f after Hillerborg [8]. The fracture energy is given by

$$G_f = \int_0^{\bar{u}_f^{pl}} \sigma_y \bar{u}^{pl} = \int_0^{\bar{u}_f^{pl}} L\sigma_y \bar{\varepsilon}^{pl} \tag{1}$$

where σ_y is the yield stress, $\bar{\varepsilon}^{pl}$ is the equivalent plastic strain, $\bar{u}^{pl}$ is the equivalent plastic displacement, i.e. the fracture work conjugate of the yield stress after onset

of damage (work per unit area of the crack) and $\bar{u}_f^{pl}$ the equivalent plastic displacement at failure. L is a characteristic length at each integration point, in this case the cube root of the integration point volume. This characteristic length is introduced to eliminate mesh dependency of results. Since the characteristic length is equal for all directions, elements with large aspect ratios will have rather different behaviour depending on the direction in which the crack occurs. Therefore the voxel approach has significant advantages over conventional meshing methods. In the present case the damage evolution is assumed to have a linear form which leads to an evolution of the damage variable

$$d = \frac{L\bar{\varepsilon}^{pl}}{\bar{u}_f^{pl}} = \frac{\bar{u}^{pl}}{\bar{u}_f^{pl}} \quad . \tag{2}$$

Where

$$\bar{u}_f^{pl} = \frac{2G_f}{\sigma_{y0}} \tag{3}$$

with σ_{y0} being the yield stress at damage initiation.

The fracture energy for mode I cracking is given in the WWFE for the unidirectional lamina as $G_f = 165\frac{\mathrm{J}}{\mathrm{m}^2}$. It is assumed that fibre breakage does not occur so that the fracture energy of the epoxy is equal to the fracture energy of the lamina.

The application of plastic deformations is physically not reasonable but has no negative consequences on the results in the present computations. A dynamic analysis is carried out to avoid numerical instabilities after the onset of damage. An explicit time integration scheme is applied using the central-difference operator. A very small loading velocity is chosen so that the dynamic effects are negligible. Furthermore very small stiffness proportional damping is applied.

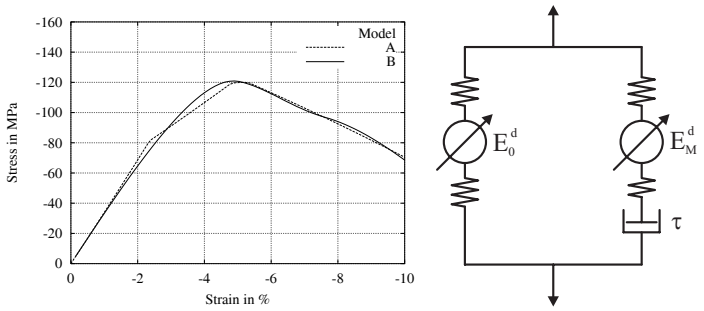

Fig. 3. Material behaviour (left) and material model B (right)

Model B: Viscoelastic regularisation

With implicit time integration numerical instabilities occur beyond the yield stress. To allow for a further computation a viscoelastic regularisation is chosen. Therefore

an elastic spring is combined with a Maxwell-element, see Fig. 3, which has in this case no physical meaning.

A visco-elasto-plastic material model with isotropic damage was developed for the computation of elastomers [12] and concrete. It distinguishes between volumetric and isochoric behaviour of the material. Through this split incompressibility of rubber and plastic incompressibility of concrete are assumed. In the following the model is described for small deformations.

Central kinematic quantity is the deformation gradient $\underline{\mathbf{F}}$. This tensor is multiplicatively splitted

$$\underline{\mathbf{F}} = (J^{\frac{1}{3}}\underline{\mathbf{1}})\,\overline{\underline{\mathbf{F}}} \tag{4}$$

into a volumetric part $(J^{\frac{1}{3}}\underline{\mathbf{1}})$ and an incompressible portion $\overline{\underline{\mathbf{F}}}$.

The fundamental constitutive equation is the strain energy function

$$\Psi = \frac{1}{2}\underline{\varepsilon}\,\underline{\underline{\mathbf{C}}}^{vd}\underline{\varepsilon} \tag{5}$$

as the function of the linear deformation tensor $\underline{\varepsilon}$ and the damaged linear viscoelastic fourth order material tensor $\underline{\underline{\mathbf{C}}}^{vd}$. Based on the split of the deformation gradient in Eq. 4 the potential function is additively composed of U, describing the hydrostatic pressure, and of an isochoric function W. The constitutive assumption of decoupled volumetric and isochoric parts

$$\Psi = U^d + W^d = (1 - d_{vol})U + (1 - d_{iso})W \tag{6}$$

yields a specific structure of the potential function. d_{vol} and d_{iso} are the volumetric and the isochoric damage variable. For elastomers $d_{vol} = 0$ is assumed.

The material tensor $\underline{\underline{\mathbf{C}}}^{vd}$ is then as well split in volumetric and isochoric parts

$$\underline{\underline{\mathbf{C}}}^{vd} = \underline{\underline{\mathbf{C}}}^{d}_{vol} + \underline{\underline{\mathbf{C}}}^{vd}_{iso}. \tag{7}$$

The volumetric part is given as a function of the volumetric Cauchy stresses $\underline{\sigma}_{vol}$ and the volumetric tangential tensor $\underline{\underline{\mathbf{C}}}_{vol}$ by

$$\underline{\underline{\mathbf{C}}}^{d}_{vol} = (1 - d_{vol})\underline{\underline{\mathbf{C}}}_{vol} - \frac{\partial d_{vol}}{\partial U}\underline{\sigma}_{vol} \otimes \underline{\sigma}_{vol}, \tag{8}$$

whereas the isochoric part

$$\underline{\underline{\mathbf{C}}}^{vd}_{iso} = \frac{E_0}{E}\underline{\underline{\mathbf{C}}}^{d}_{iso} + \frac{E_M}{E}\frac{\tau}{\Delta t}\left[1 - \exp\left(-\frac{\Delta t}{\tau}\right)\right]\underline{\underline{\mathbf{C}}}^{d}_{iso} \tag{9}$$

is the addition of the tangent tensors of spring- and Maxwell-element. The variable E is the overall stiffness and E_0 the stiffness of the spring, see Fig. 3, τ and E_M are the relaxation time and the stiffness of the Maxwell-element, respectively. The elastic isochoric material tangent $\underline{\underline{\mathbf{C}}}^{d}_{iso}$ is a function of the deviator of Cauchy stresses $\underline{\sigma}$ and the isochoric tangential tensor $\underline{\underline{\mathbf{C}}}^{e}_{iso}$ and yields

$$\underline{\underline{\mathbf{C}}}^{d}_{iso} = (1 - d_{iso})\underline{\underline{\mathbf{C}}}^{e}_{iso} - \frac{\partial d_{iso}}{\partial W}\mathrm{dev}\underline{\sigma} \otimes \mathrm{dev}\underline{\sigma} \quad . \tag{10}$$

Material Parameters

The material parameters shown in table 2 are taken from the WWFE [9]. The volume fraction of the lamina is given as $V_f = 60\%$.

Table 2. Mechanical properties of fibre and matrix

Properties	Unit	Silenka E-Glass 1200 tex	MY750/HY917/DY063 epoxy
Modulus	GPa	74	3.35
Strength	MPa	2150/1450[1]	80/120[1]
Failure strain	%	2.950/1.959[1]	5/–[1]
Shear Modulus	GPa	30.8	1.24
Poisson's ratio		0.2	0.35

[1] tensile/compressive

Discretisation

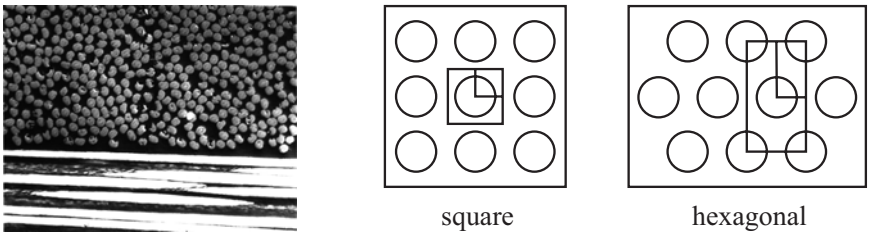

Fig. 4. Micrograph (left) and assumed arrangement of fibres for RVEs

The formation of fibres is far from being regular, for RVEs there are often two different approximations used: square and hexagonal arrangement, see Fig. 4. In Fig. 5 different discretisation levels for square and hexagonal arrangements are shown. With the perspective of using the same model for textile composites volume elements are used and the mesh always is one element thick. The discretisation is equal for both material models. Instead of a conformal mesh an approximate mesh is used. It does not attempt to exactly match the geometry of the RVE, which is, by the way, only an assumption. The RVE of an approximate mesh is subdivided in elements of the same size with an aspect ratio of unity, called "voxel" (a volume pixel). The voxel approach has a number of advantages that mainly derive from the fact that especially with more complicated geometries many deformed elements appear in conformal meshes:

- Deformed elements have a negative influence on the performance and results of the finite element method.

- The fracture energy formulation of model A works badly with deformed elements, see Sect. 2.4.1.
- Periodic boundary conditions are much easier to apply on matching opposite faces of the RVE.

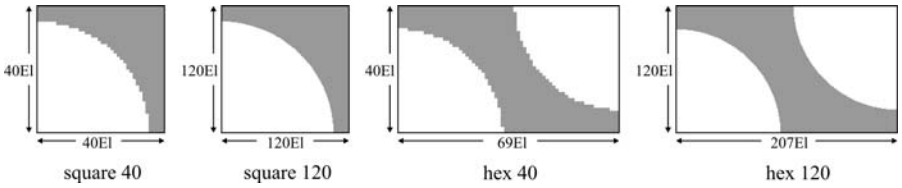

Fig. 5. Discretisation levels

For the determination of material properties four different load cases are considered, see Fig. 6. Loads were applied displacement driven, because force-driven load application fails beyond the point of maximum load. The necessary periodic boundary conditions are chosen according to [19], except for transverse shear. For each normal load case all RVE faces are forced to stay even and parallel. The boundary conditions for shear loading are derived out of the transversely isotropic material symmetry of an UD-lamina. In-plane shear involves two different directions and is therefore modeled as simple shear. In contrast to [19] transverse shear is modeled as pure shear, because it involves two similar directions. For better understanding of the ongoing deformations under shear Fig. 7 shows the in-plane shear deformation of a hexagonal RVE on the left and the transverse shear deformation of a square RVE on the right.

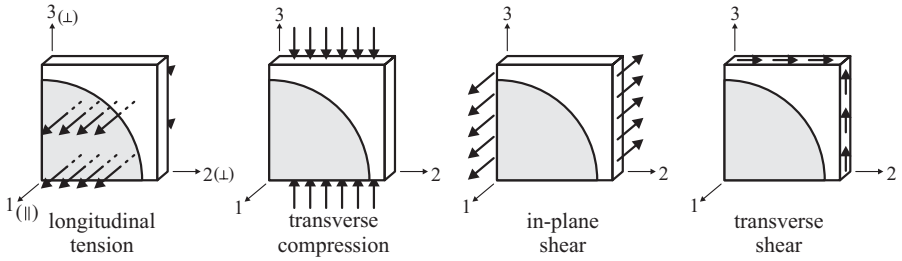

Fig. 6. Different loading conditions

2.4.2 Transverse compressive strain

In the WWFE [9] the nonlinear behaviour of UD-laminae under transverse compressive strain is given. These experimental results are compared to RVE computations in Fig. 8. The most noticeable result is the difference between the stiffnesses

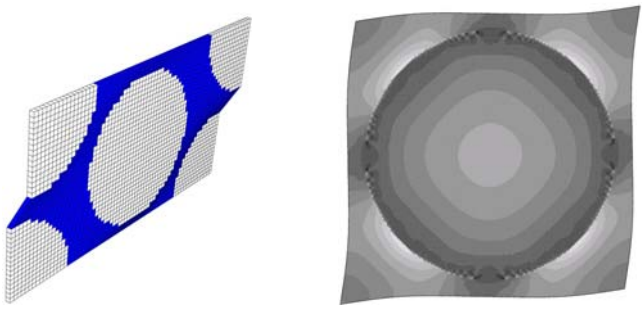

Fig. 7. Deformations caused by in-plane shear (left) and transverse shear (right)

of square and hexagonal arrangement. This has as well been observed in other publications [5][19] and will be discussed in detail in the next paragraph. Both models show good convergence. The fracture energy terms in model A and the viscoelastic regularisation in model B are responsible for this good convergence behaviour. However, model B obviously describes the nonlinear material degradation and thus also the strength better than model A. The square arrangement matches the test results nearly perfect. It can be concluded that the strain energy-dependent damage variable of model B is considerably a more reasonable description for material degradation than the plastic formulation with isotropic hardening of model A.

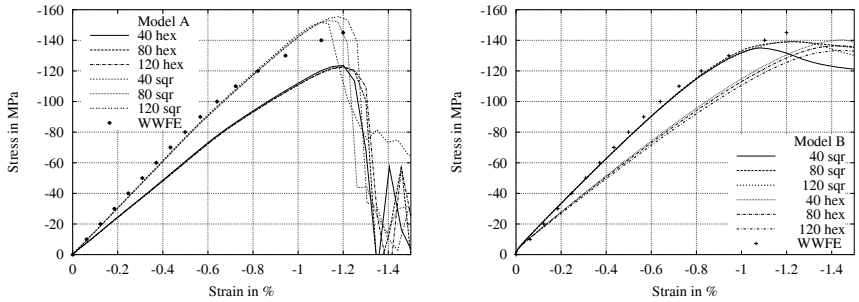

Fig. 8. Transverse compressive strain, model A (left) and model B (right)

Different stiffness of arrangements

Obviously the square arrangement is stiffer than the hexagonal arrangement. This can be easily understood when looking at the RVEs in Fig. 9. Both RVEs have the same fibre volume fraction of $V_f = 60\ \%$. For transverse compression fibre and matrix can be seen as series springs. The fibre is stiffer than the matrix by an order of magnitude, therefore the matrix is mainly responsible for the transverse stiffness. In the square arrangement the radius of the fibre is greater, i.e. the proportion of the

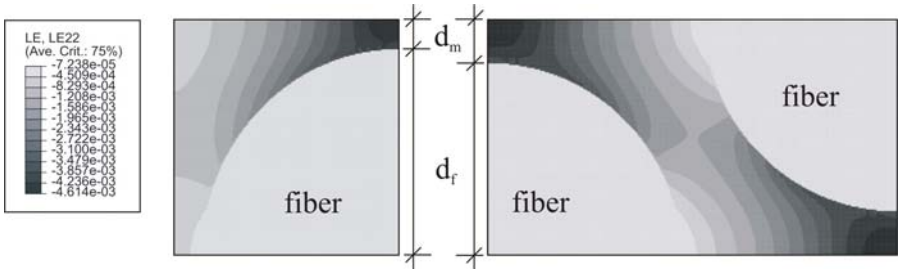

Fig. 9. Strain distribution in square and hexagonal arrangement of RVE

matrix d_m in load-direction is smaller. Hence the square-packed RVE is stiffer than the hexagonal-packed RVE. The strain distributions in Fig. 9 show the relevance of this fibre to matrix proportion.

2.4.3 Influence of fracture energy

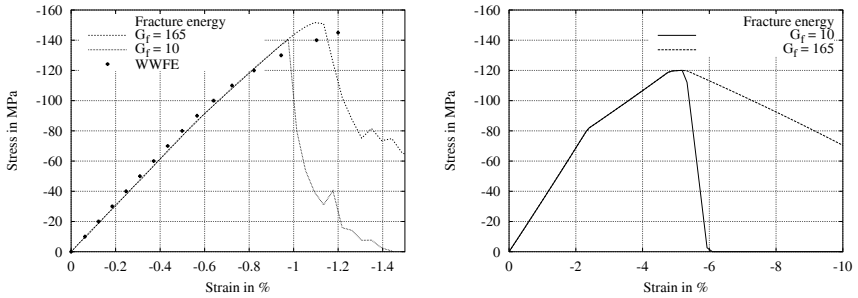

Fig. 10. Influence of fracture energy on RVE (left) and matrix material behaviour (right)

It may be argued that it is sufficient to determine failure of RVEs via the maximal stresses or strains of the matrix. The computational effort could easily be reduced by such an procedure, but, as Fig. 10 shows, it provides by far too conservative results. Fig.10 shows stress-strain curves computed with Model A for different fracture energies. On the left side a stress-strain curve for a RVE under transverse compressive strain and on the right the stress-strain curve of the epoxy matrix are shown. Using the measured fracture energy $G_f = 165\frac{J}{mm^2}$ yields a good agreement with experimental results, whereas $G_f = 10\frac{J}{mm^2}$, representing a brittle matrix, results in clearly too small failure stress and strain. A realistic fracture energy in the present case allows for load redistribution and thus realistic strength. Therefore it is very important to apply continuum damage mechanics in the strength computation of RVE models.

2.4.4 Results

Results for all load cases of Fig. 6 are summarised in table 3 for square and hexagonal arrangements of model A and model B. The test results are given in the WWFE [9]. Table 3 shows that the differences between square and hexagonal arrangements are quite considerable and it can not be concluded that one of these approaches provides better results than the other. Consequentially a probabilistic evaluation of different RVE arrangements might yield good results.

Under in-plane shear the UD-lamina exhibits pronounced nonlinear behaviour, see Fig. 2. Therefore further studies with a better description of the nonlinear behaviour of the epoxy are planned. The given material parameters are obviously not sufficient for a reliable prediction in this load case. The applied RVEs are not capable of predicting fibre kinking under longitudinal compression. This phenomenon is massively influenced by fibre waviness and can only be analysed with RVEs on a greater scale.

Table 3. Mechanical properties E-Glass MY750/HY917/DY063-epoxy lamina

Properties	Unit	Test results	Hexagonal	Square
Longitudinal modulus[1] $E_{\parallel}$	GPa	45.6	45,7	45,7
Longitudinal tensile strength $R^{t}_{\parallel}$	MPa	1280	1308	1308
Longitudinal tensile failure strain $\varepsilon^{t}_{\parallel}$	%	2.807	2.94	2.94
Transverse modulus[1] $E_{\perp}$	GPa	16.2	12.1/11.2[2]	15.2/15.1[2]
Transverse compressive strength $R^{c}_{\perp}$	MPa	145	122.9/132.0[2]	156/139.2[2]
Transverse compressive failure strain $\varepsilon^{c}_{\perp}$	%	1.2	1.2/1.46[2]	1.18/1.22[2]
In-plane Shear Modulus[1] $G_{\parallel\perp}$	GPa	5.83	4.43/4.41[2]	4.68/4.68[2]
In-plane Poisson's ratio $\upsilon_{\parallel\perp}$		0.278	0.251	0.249
In-plane Shear Strength $R_{\parallel\perp}$	MPa	73	–[3]	–[3]
In-plane Shear failure strain $\upsilon_{\parallel\perp u}$	%	4	–[3]	–[3]
Transverse Shear Modulus[1] $G_{\perp\perp}$	GPa	–	3.63	3.27
Transverse Poisson's ratio $\upsilon_{\perp\perp}$		0.4	0.39/0.33[2]	0.26/0.24[2]
Transverse Shear Strength $R_{\perp\perp}$	MPa	–	–[3]	–[3]
Transverse Shear failure strain $\upsilon_{\perp\perp u}$	%	–	–[3]	–[3]

[1] Initial modulus
[2] Model A/Model B
[3] Still under investigation

2.5 Standards for experimental evaluation of composites

There are numerous experimental tests defined and evaluated for composites. Generally it is sophisticated to define a standard test procedure for composites, because of the complex anisotropic material characteristic and failure behaviour of prepreg and especially textile composites. Nevertheless, there are tests established to determine the basic material parameters for prepregs.

Usually the in-plane material properties are determined by coupon tests on lamina as well as laminate level. For the former coupons are cut from thin, unidirectional plates with a material thickness of approximately 2 mm according to the specified test setup. Commonly a standard tensile testing machine is used to determine the material parameters. For the tensile and compressive properties of a single ply, 0°- and 90°-specimens are used. Additionally the shear properties are determined by a tensile test with a laminate lay-up of $\pm 45°$. Unfortunately this test provide material parameters of a laminate which are probably characteristic to a shear deformation of a single UD ply, but strictly speaking in comparison with the ideal pure shear loading within a RVE model a different stress state and material is evaluated. Nevertheless, 5 different material properties are determined, which allow to calculate the transversely-isotropic material stiffness.

Although the stiffness of the laminate is approximately determinable by the classical laminate theory, the failure of the laminate is based on a complex failure process and requires additional properties. Furthermore the behaviour of a single ply is supposably different to an embedded ply in a laminate and the free-edge effect influences the failure load, which is especially important for the validity of coupon specimen tests. Additional effects concerning the material lay-up, the specimen manufacturing, the material fabrication and environmental conditions scatter the testing data and result in uncertain material strength values. Hence, it is obvious that testing of composites with coupon specimen is a complex field of research.

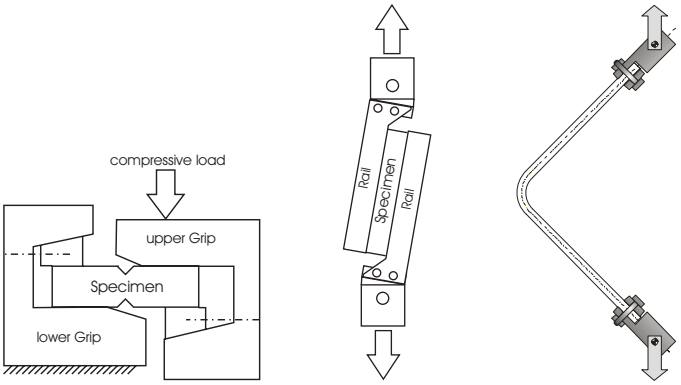

Fig. 11. Isoipescu, Two-Rail shear and L-Beam test

Additional test setups are developed, especially to evaluate shear loading of unidirectional lamina, particularly according to the problems with the standard shear test on coupon level. The rail shear test is used to introduce shear loads by a tensile deformation of two or three rails. The Isoipescu-test provides a shear load by introducing in-plane transversal compressive loads in a v-notched specimen geometry (Fig. 11). The most useful test is probably a torsional deformation of a tubular specimen, because the free edges are minimised and the stress state is nearly pure shear. There are

a lot of further tests available to determine the basic material properties of unidirectional lamina, for example a twisting plate test, deformation of closed ring or a ring with a cutout and various specific flexure tests like the L-Beam test. A numerous of standard tests and a convenient overview is provided by Hodgkinson [10].

Additional tests are more interesting to validate numerical models, analysis procedures or failure theories. Therefore the material behaviour has to be evaluated by multiaxial loads. Appropriate tests are for instance the flexure test of a beam or the combined loading of a tubular specimen. Extensive test results for prepreg composites are achieved by the World-Wide-Failure-Exercise [9], where internal or external pressurised tubular specimens were tested with axial or torsional loads. The results of these tests provide the potential to evaluate the quality of the failure prediction based on the RVE models.

3 Textile Composites

3.1 Fabrication and material characteristics of Textile Composites

Prepreg composites probably utilise the fibre properties optimal, whereas the manufacturing and material cost are disadvantageous for industrialised high volume productions. Due to reduced manufacturing and material costs textile composites are potentially cheaper. Hence, these materials are interesting for structures where high mechanical properties with a low-cost material are required.

3.1.1 Types of textile composites

There are various types of textile composites in common use with different textile architectures. Continuous aligned fibre textiles for lightweight structures can generally be categorised in four main groups:

- Braided Fabrics,
- Woven Fabrics,
- Non Crimp Fabrics,
- Filament winding composites.

Basically, for high performance structures, fibre architectures are considered, which are rather capable of utilising the full fibre potential. Therefore textile architectures without continuous fibre directions, like knitted fabric reinforcements or randomly oriented milled fibre composites, are considerably uninteresting.

Braided composites are produced by interlacing reinforcement fibres around a certain geometry. A tow, which is a bundle of filaments in an untwisted configuration is wound around a mandrel and interlaced with a certain number of additional tows. The triaxial braid provides a third tow parallel to the component axis. With the braiding technology a characteristic pattern of tows around the mandrel is formed. These textile raw materials are commonly used for tubular, relatively long components like bars, cantilevers beams and tubes. Generally, this two dimensional braiding architecture is similar to woven textiles except that it encircles a tubular component.

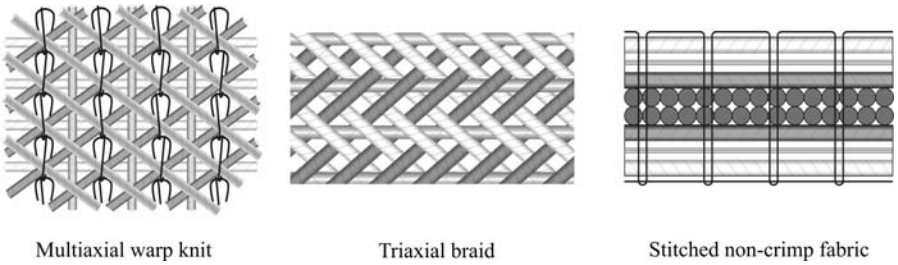

Fig. 12. Textile fiber architectures

Woven textiles are produced with various weave styles. They are supplied on a roll and their plane geometry can be formed to a three dimensional shape with relative ease as far as the required deformation is not too large. The fibre tows are interwoven with each other and therefore exhibit crimps. These small periodical fibre misalignments are commonly described as fibre undulations. For woven composites it is generally accepted that the presence of undulations reduces the in-plane mechanical performance. Different textile architectures or weave styles are producible, which generally exhibit different material characteristics and manufacturing restrictions. Generally they are categorised according to their producibility and mechanical performance.

Generally textile fabrics and woven composites are manufactured by a process, wherein a warp thread is woven with a weft thread. Obviously this process leads to small periodical fibre misalignments on a micromechanical level due to interlacing of crossing tows. These misalignments decrease the in-plane material properties. The basic idea of non-crimp fabric materials is to align the fibres in a precise continuous orientation with as less as possible undulations. Non-crimp fabric (NCF) reinforcements are manufactured by placing tows at the required orientations in discrete layers and stitching them together using a lightweight textured polyester thread. In the optimal case the stitching thread dissolves in the resin system during the curing process and the reinforcement fibres remain in a straight-lined orientation. These reinforcements are generally considered to offer mechanical properties superior to those available from woven reinforcements since the tows remain straight. Nevertheless, it is assumed that the material properties of NCF materials are significantly lower due to the fibre waviness compared to prepregs. Concerning textile composites the NCF material provides probably the highest potential for the construction of lightweight structures. Therefore it is a interesting prospect to analyse the NCF material by an enhanced experimental evaluation and numerical models on micromechanical level.

The most accurate fibre orientation is provided by the filament winding technology. Generally the winding process can be used for prepregs as well as dry textile tows and is not restricted to substantially infusible dry textile composites. This process is used for fabricating of composites in which continuous reinforcing fibres, either preimpregnated with resin or drawn through a resin bath, are wound around a

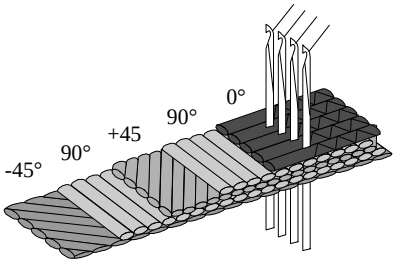

Fig. 13. Multiaxial non-crimp fabric

rotating, removable mandrel. A certain stitching yarn or interwoven configuration is not required and the fibre orientation is continuous straight-lined. Therefore the mechanical properties are similar to prepregs but the geometry is restricted according to the producibility of the winding technology.

3.1.2 Manufacturing of textile composites

Opposed to pre-impregnated composites, the textile preform in form of a braided, woven, stitched or wound textile is generally impregnated by the resin system. The liquid resin infusion method (LRI) provides a significant reduction in manufacturing cost compared to the prepreg production in which therefor a high component quality is attained by compacting the prepregs in the autoclave. Nevertheless, the autoclave assisted manufacturing is disadvantageous concerning high volume applications and leads to high material costs.

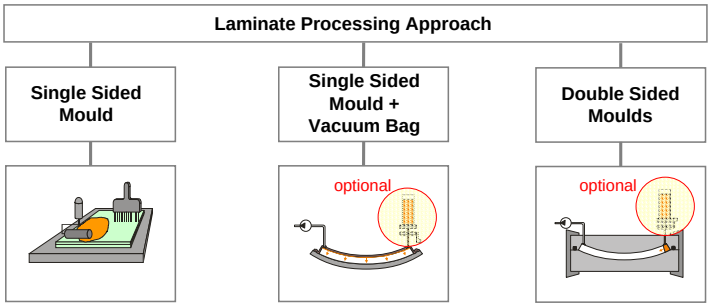

Fig. 14. Liquid resin infusion processes for textile preforms [14]

The liquid resin infusion processes can be classified according to the resin impregnation technique and tooling. The traditional method is known as hand lay-up, in which a dry fibre reinforcement preform is cut to the desired shape and placed in a simple one sided mould. Resin systems are applied in liquid form to the preform by hand. The lamina is compacted by a roller and cured under ambient temperature

or in an oven. This process enable a very low cost tooling but is restricted to a relatively low fibre volume fraction and material quality according to unprecise fibre orientations, undulations and void entrapments. Hence, this process is comparatively unimportant for the production of high performance structures.

The vacuum assisted infusion technology provides a closed mould and higher fibre volume fractions compared with the hand lay-up. The production procedure is slightly reminiscent to the prepreg process, in which the preform is assembled in a single sided mould and sealed under a vacuum bag. The resin is injected in the system at atmospheric pressure through an inlet and flows through the preform to the vent. Because of the low tooling cost and the environmental producibility this process is established for the production of large components and structures such as boat hulls and future airplane fuselage. Additionally the process is promoted by the ability to make high quality parts with low void content and high fibre volume fraction.

The resin transfer moulding (RTM) process provides relatively good material quality but requires expensive tools. Especially the production of high volume applications legitimate therefore the RTM process. In the RTM process a dry textile preform is placed between a pair of rigid moulds, which are usually from metal. The liquid resin is injected under pressure and flows through the cavity of the mould towards a vent, which is maintained at atmospheric or lower pressure. The parts produced by this process have excellent dimensional accuracy, surface finish and a high potential for good mechanical properties and reproducible quality. Although only smaller parts are producible than with the vacuum bag assisted injection, the RTM process is used extensively for commercial production, especially in the automotive industry.

There are additional processes for the infusion of textile composites with more or less greater modifications on the above described technologies. An advanced interesting possibility provide the autoclave assisted injection, for example the single line injection (SLI) process, which was developed at the DLR [7]. The SLI process is a vacuum assisted infusion process in combination with an autoclave to assure a precise fibre volume fraction and minimal fibre undulations provided by a low-cost tooling using a single sided mould.

Generally textile composites provide the possibility to integrate different components in one structure. This enables the possibility to reduce manufacturing cost, material amount, and weight of a structure. Therefore textile structures are provide an interesting prospect for lightweight and economical structures. A detailed evaluation of the NCF material is a essential step towards a qualified application to high performance lightweight structures. Thereby the analysis on a micromechanical level seems to be a promising method, particularly for the stiffness and strength prediction of three dimensional reinforced NCF materials.

3.1.3 Material characteristics of textile composites

The material behaviour of textile reinforced composites is based on a multitude of effects and is generally different from the behaviour of prepreg or filament winding

composites, in which the fibres are aligned in a nearly perfect, continuous, undisturbed direction. It is mostly assumed that the material symmetry can be modeled with regard to a transversely-isotropic material symmetry. Properly aligned prepreg laminates and filament winding composites approximately provide this material symmetry on the lamina level. Although the progressive failure of an unidirectional composite already degrades the material symmetry by an onset of cracks at small loads, this approximation is probably useful for the meso-mechanical analysis of a lamina with nearly perfect fibre distributions. Opposed to this approximation textile composites are characterised by fibre waviness, due to the woven, braided or stitched preform of the dry raw material. This fibre undulation is characteristic for textiles and substantial for the mechanical behaviour, especially for the failure analysis.

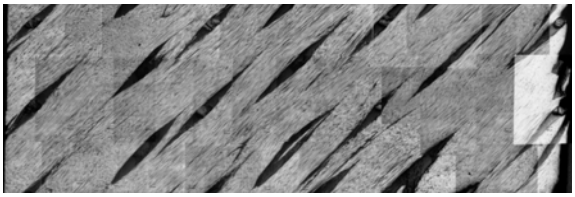

Fig. 15. Fibre waviness and resin pockets on micromechanical level (undulations) of a stitched NCF [18]

Because textile composites are manufactured with relatively large fibre tows which are interwoven or stitched in geometric complex patterns, they contain significant volumes of resin pockets, which are recognisable in Fig. 15 as black areas. Although this resin rich zones are negligible for the macroscopic stiffness analysis, their influence on the strength and failure mechanic is of most relevance. Especially the thermal expansion of the resin due to the curing and post-curing process causes a resin shrinkage in the cured composite. The relatively stiff fibres with a lower thermal expansion, especially carbon fibres, resist the resin shrinkage. Therefore, residual stresses arise in the material microstructure, which could result in cracks and microstructure defects of the composite. In this regard infusible resin systems are particularly critical because of their brittle mechanical failure behaviour. The infusible resin is optimised for a certain viscosity and provide usually lower allowable strains compared with the resin system used for prepregs.

Generally fibre waviness and resin rich zones are caused by the braiding and weaving as well as the stitching process. It was proven [18] that stitched non-crimp fabrics provide an increased delamination strength compared with unstitched specimens and especially prepreg systems. This advantage is often more important for integrating components into a larger structure by stitching them together, even though cracks arise in the resin rich zones on the microscopic level (Fig. 16) due to an increasing fibre waviness.

Even if the stitching process is able to increase the out-of plane strength it is proven that the in-plane properties are usually decreased. The failure behaviour of a

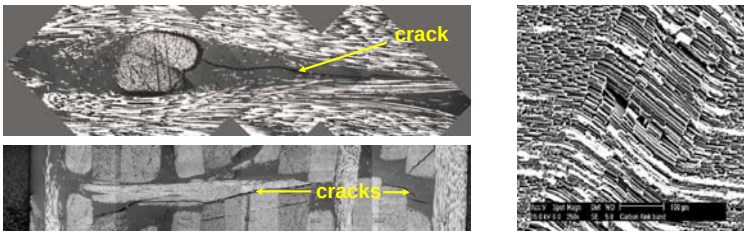

Fig. 16. Microcracks in a stitched textile composite [18] (left), Fibre kinking [1] (right)

stitched textile is more complex due to (excessive) arising cracks and microstructural defects. Nevertheless, the impact and crash tolerance is enhanced by the stitching process. The compression strength is generally reduced by stitching because the in-plane fibres are often misaligned in a periodical pattern. If this affects an entire ply of fibres, it could result in a compression buckling phenomenon of that ply, which is commonly described as a fibre kinking effect. Due to the increased fibre waviness it is obvious that the kinking failure is more critical for textiles rather than prepreg or filament winding composites.

Commonly the elastic behaviour of composites is described by linear elastic constitutive equations up to the first-ply failure of a laminate. Beyond the determination of the first-ply failure, it is probably essential to describe the behaviour of textiles by nonlinear models. This nonlinear behaviour results from accumulated microstructural defects by monotonically increasing loads. Furthermore the microstructural defects allow for a fibre realignment, in which the fibre undulations decrease in the load direction. Therefore, this failure behaviour is dependent on the textile architecture and results in a macroscopic non-linear material behaviour. The microstructural defects arise on very small macroscopic strain levels unless they are already present from the curing process in consequence of residual thermal stresses. The understanding of these micromechanical failure processes is an essential part in developing accurate failure criteria and stiffness prediction of laminated textile composites. Thus micromechanical approaches which are capable of covering fabrication defects are required.

3.2 Research activities on the mechanical behaviour of textile composites

Research activities on mechanical behaviour of textile composites can be categorised mainly in two groups, RVE and phenomenological models.

3.2.1 RVE models

The first main difficulty in characterising the mechanical behaviour with RVE models is to account for the geometric discontinuities in the fibre architecture, see Sect. 3.1.3. Second main difficulty are of course the probabilistic deviations of the component from the idealised RVE. This more general problem of every RVE approach arises

especially for textile composites, because of the comparatively bad reproducibility described in Sect. 3.1.2. Another probabilistic factor are defects like microcracks from e.g. residual thermal stresses resulting from the fabrication process or moisture effects. Analytical models have been developed, but these always require assumptions on the stress or strain fields, which can be seen as a limitation. The application of numerical models overcomes this disadvantage, the main difficulty though remains the geometric structure of textile composites. An exact representation of a three-dimensional RVE often involves a great number of elements of which many have deformed shapes. However, deformed element shapes violate the assumptions of the finite element method. Furthermore, the application of periodic boundary conditions for shear requires matching of opposite faces of the RVE. Conventional finite elements have been used by a number of research groups for the prediction of stiffnesses. Other approaches have been developed which mainly deal with the problem of mesh generation and reduction of numerical costs. A small selection is described subsequently.

Wisetex

A tool has been developed by Lomov et al. [16] for the generation of various fibre geometries. It can create 3D images of the fabric and import the fabric data into flow simulation software for prediction of the fabric air- or resin-permeability, import the fabric data into micromechanics simulation software for prediction of stiffnesses and import the fabric data into finite element packages.

Binary Model

This method, proposed by Cox et al. [2] discretises the fibre tows as one-dimensional truss elements which are connected to the matrix discretised as volume elements through multi-point-constraints. Therefore the matrix can be discretised with regular elements and the waviness of the tows is nonetheless represented very exact by the truss elements. The method predicts the elastic behaviour with little computational effort. It has been taken up by Haasemann and Ulbricht [6] to compute material parameters for a cosserat continuum element which accounts for the different elastic moduli of textile composites in normal and bending loading.

Voxel approaches

The voxel approach has been described and used above, see Sect. 2.4.1. It has been thoroughly tested by Gunnion [5] for the stiffness prediction of textile composites. Kim and Swan [13] introduce a mesh refinement technique based on voxel elements. They replace voxel elements at the boundaries between fibre and matrix by refined voxel meshes and introduce multi-point-constraints to ensure continuity of the mesh.

3.2.2 Phenomenological models

Approach for layered textile composites with orthogonal reinforcements

A summary of phenomenological failure criteria based on the fracture plane concept for Prepreg-laminates is given by Cuntze et al. [4]. Amongst others the simple parabolic criterion is discussed, that is a stabilisation and simplification of Puck's parabolic criterion described in Sect. 2.3. Juhasz et al. [11] adapt the simple parabolic criterion to inter-fibre failure of orthogonal 3D fibre reinforced plastics although the fracture angle concept for such a geometry yields only one possible fracture plane. Moreover, due to the complex failure behaviour of textile composites it is almost impossible for 3D reinforced structures to detect a fracture plane or to even measure a fracture angle in experiments. Nevertheless, Juhasz brings forward the argument that the fracture angle concept has to be understood as an extremum principle, where the fracture angle determines the plane of the first occurrence of IFF. This criterion was implemented in a three dimensional finite element to account for the three dimensional stress state in each layer of a lamina by Kuhlmann and Rolfes [15]. The strengths of the failure plane R_N, R_{NT} and R_{NL} are given by

$$R_N^{(+,-)} = \tilde{R}_y^{(+,-)} sin^2\theta + \tilde{R}_z^{(+,-)} cos^2\theta + \tilde{R}_{yz}^{(+,-)} |sin2\theta| \quad , \tag{11}$$

$$R_{NT}^{(+,-)} = \left(\tilde{R}_y^{(+,-)} + \tilde{R}_z^{(+,-)}\right) |sin2\theta| + \tilde{R}_{yz}^{(+,-)} \quad , \tag{12}$$

$$R_{NL}^{(+,-)} = \tilde{R}_{xy}^{(+,-)} |sin\theta| + \tilde{R}_{xz}^{(+,-)} |cos\theta| \quad . \tag{13}$$

The strength parameters $\tilde{R}_y, \tilde{R}_z, \tilde{R}_{yz}, \tilde{R}_{xy}and\tilde{R}_{xz}$ can be derived via a fitting procedure described in [11] from off-axis tests. However, the specimens for these tests are hardly producable, so the determination of strengths with finite element RVE model is an attractive alternative.

3.3 Mesomechanical RVEs for layered textile composites with orthogonal reinforcements

It is hardly possible to experimentally determine the through thickness properties of textile composites, therefore RVE models are an attractive alternative. In this section an RVE approach for the determination of strength parameters for a phenomenological failure criterion is introduced.

RVE models for textile composites have to be applied on a greater length scale than the previously shown micromechanical RVEs for UD-laminae in Sect. 2.4. In textile composites the fibres are arranged in tows, which include parallel aligned fibres in an epoxy matrix and are similar to UD-laminae. However, the RVE has to model the geometric arrangement of the tows and resin pockets. The tows are assumed to be transversely isotropic and, due to the lack of a more precise material model, linear elastic. Material parameters are taken from the micromechanical prepreg analysis with hexagonal arrangement given in table 3. The epoxy resin is modeled with model A of Sect. 2.4.1.

Fig. 17 shows the RVE for a layer of a textile composite with orthogonal reinforcements on the left side. This RVE is thought to be an approximation for a lamina of a NCF. It neglects possible imperfections which will be implemented in further investigations. The RVE has two tows with a volume fraction of $V_f = 50\%$ and a weak orthogonal reinforcements with a volume fraction $V_f = 1\%$. NCFs usually have higher volume fractions, but because only matrix cracking is considered here, a lower volume fraction is preferred in this example. Fig. 17 also shows stress-strain curves of normal and shear loads applied on the RVE. The strengths and failure strains can be taken form the curves and then be applied in the failure criterion of Juhasz, see Sect. 3.2.2.

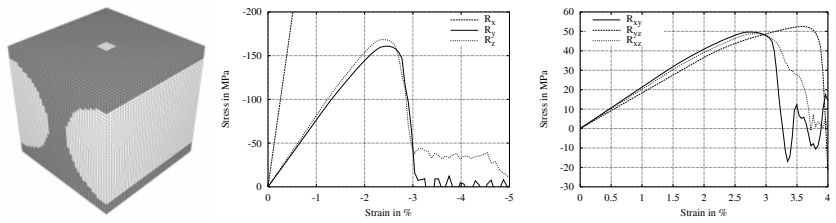

Fig. 17. 3D RVE (left) and basic strengths of layer

Figs. 18 and 19 illustrate the cracking of the epoxy resin. Black areas are fully damaged. The load direction is given in the pictograms on the left, the RVEs are rotated in such a way that the load direction is always the same for the reader. Fig. 18 shows the results of three compression load cases. The crack distributions in load case 2 and 3 resemble inter-failure under crack mode $\sigma_{\perp}^{(-)}$ of Puck's fracture plane concept in Fig. 1, whereas compression in main tow direction might give an indication for fibre kinking. Three shear load cases are shown in Fig. 19. Unlike UD-lamina textile composites don't possess a $\tau_{\perp\perp}$-plane. The fracture plane always remains parallel to the main fibers, the orthogonal reinforcement is cut by the fracture plane, though.

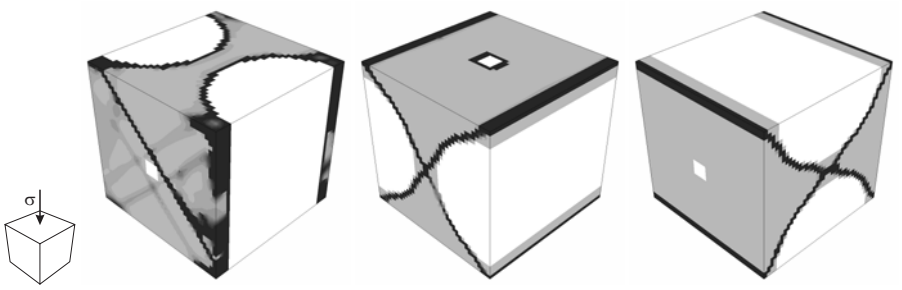

Fig. 18. Normal deformations under vertical compression, tows in white, damage in black

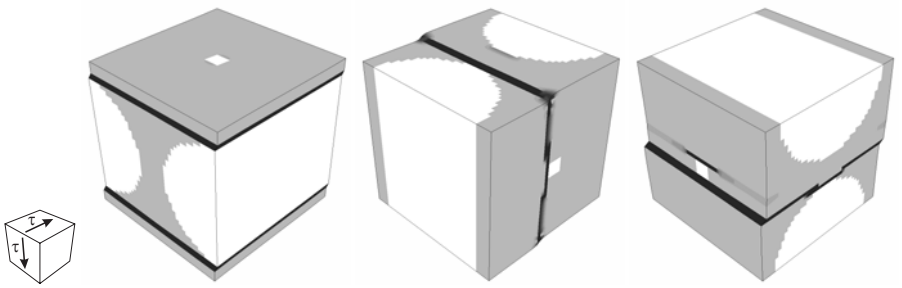

Fig. 19. Shear deformations, tows in white, damage in black

4 Conclusion and outlook

From the comparison of two different material models it can be concluded that the strain energy damage variable formulation is very good for the prediction of material nonlinearities. It has also been shown that the fracture energy formulation provides a good convergence of results. The viscoelastic regularisation has proven to work reliably for numerical stabilisation.

Significant differences in the results of square hexagonal arrangement RVEs have been found. It has been shown that the consideration of the fracture energy is necessary for a realistic RVE failure computation. The results of shear failure are hardly to determine without a good description of epoxy material. Under normal loading the proposed RVEs are able to provide a good prediction of failure.

Outlook

The RVE model will be extended for the consideration of fibre waviness and thermal stresses. For the improvement of shear failure prediction realistic epoxy material behaviour will be implemented. An anisotropic damage for anisotropic materials is of most relevance for the RVEs of textile composites. Very promising with respect to the differences between square and hexagonal arrangement is a probabilistic evaluation. The influence of geometric imperfections and pre-existing defects will be analysed. The results from the mesomechanical RVEs are to be compared to experimental results.

Acknowledgements

Part of this work was funded by the German Research Council (DFG). This support within the framework of SPP-1123 ‘Textile composite design and manufacturing technologies for lightweight structures in mechanical and vehicle engineering’ is highly appreciated.

References

1. Basu S, Waas AM, Ambur DR (2006) Compressive failure of fiber composites under multiaxial loading. Journal of the Mechanics and Physics of Solids 54:611 — 634
2. Cox BN, Carter WC, Fleck NA (1994) A binary model of textile composites- I. formulation. Acta metall. mater. 42(10):3463 – 3479
3. Cox BN, G. Flanagan (1997) Handbook of Analytical Methods for Textile Composites. Materials Sciences Corporation, Prepared for Langley Research Center, Philadelphia, Pennsylvania
4. Cuntze R (ed) (1997) Neue Bruchkriterien und Festigkeitsnachweise für unidirektionalen Faserkunststoffverbund unter mehrachsiger Beanspruchung – Modellbildung und Experimente –. VDI-Verlag, Düsseldorf
5. Gunnion AJ (2004) Analytical assessment of fibre misalignment in advanced composite materials. PhD thesis, RMIT University, Melbourne
6. Haasemann G, Ulbricht V (2005) Flexural properties of fiber-reinforced composites. Proceedings in Applied Mathematics and Mechanics 5(1):233 – 234
7. Herrmann AS, Pabsch A, Kleineberg M (2001) SLI-RTM Fairings for Fairchild Dornier DO 328 Jet. Proceedings SAMPE EUROPE Conference, SAMPE, Paris
8. Modeer M, Hillerborg A, Petersson PE (1976) Analysis of crack formation and crack growth in concrete by means of fracture mechanics and finite elements. Cement and Concrete Research 6:773—-782
9. Hinton MJ, Kaddour AS, Soden PD (eds) (2004) Failure criteria in fibre reinforced polymer composites: The World-Wide Failure Exercise. Elsevier Science, Oxford
10. Hodgkinson JM (ed) (2000) Mechanical testing of advanced fibre composites. Woodhead Publishing Limited, Abington Hall, Cambridge
11. Juhasz TJ, Rolfes R, Rohwer K (2001) A new strength model for application of a physically based failure criterion to orthogonal 3D fiber reinforced plastics. Composite Science and Technology 61:1821 – 1832
12. Kaliske M, Nasdala L, Rothert H (2001) On damage modelling for elastic and viscoelastic materials at large strain. Computers and Structures 79:2133–2141
13. Kim HJ, Swan CC (2003) Voxel-based meshing and unit-cell analysis of textile composites. International Journal for Numerical Methods in Engineering 56:977–1006
14. Kleineberg M, Herbeck L, Schöppinger C (2002) Advanced liquid resin infusion - A new perspective for space structures. European Conference on Spacecraft Structures, Materials and Mechanical Testing, Toulouse, France
15. Kuhlmann G and Rolfes R (2004) A hierarchic 3d finite element for laminated composites. International Journal for Numerical Methods in Engineering 61:96–116
16. Lomov SV, Belov EB, Bischoff T, Ghosh SB, Truong Chi T, Verpoest I (2002) Carbon composites based on multiaxial multiply stitched preforms - Part 1. Geometry of the preform. Composites Part A: Applied science and manufacturing 33:1171—1183
17. Puck A (1996) Festigkeitsanalyse von Faser-Matrix-Laminaten, Modelle für die Praxis. Carl Hanser Verlag, München
18. Sickinger C, Herrmann AS (2001) Structural stitching as method to design high performance composites in future. Proceedings TechTextil Symposium 2001, Messe Frankfurt, Frankfurt am Main
19. Sun CT, Vaidya RS (1996) Prediction of composite properties from a representative volume element. Composites Science und Technology 56:171–179